JP&M Engineering
Journal of Petroleum and Mining Engineering

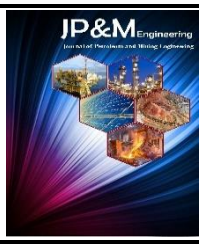

Modern Decline Curve Analysis of Unconventional Reservoirs: A Comparative Study Using Actual Data

Wahba, A. M. *, Khattab, H. M., Tantawy, M. A., Gawish, A. A.
Petroleum Engineering Department, Faculty of Petroleum and Mining Engineering, Suez University, Suez, Egypt
*Corresponding author e-mail: a.wahba@suezuni.edu.eg

Article Info

Received 18 Mar. 2022
Revised 27 Apr. 2022
Accepted 29 Apr. 2022

Keywords

Unconventional reservoir; decline curve analysis; hydraulic fracturing; field data; comparison.

Abstract

Petroleum consumption increases around the world and production of conventional reservoirs can't cover the increased demand. So, producing unconventional resources is an imperative necessity. Unconventional resources are characterized by very low permeability. Drilling horizontal wells in these resources and completed them with multiple hydraulic fractures make the reservoir. Hydraulic fractures work as paths for hydrocarbon to flow toward the wellbore to achieve an economic production rate. Production behaviour of these wells is characterized by long-term transient flow followed by boundary-dominated flow. Many decline curve analysis models have been developed to simulate this behaviour, but none of them can capture all flow-regime types. This paper reviewed the most popular and used decline curve analysis models: Arps model, power-law exponential model, stretched exponential production decline model, T-model, logistic growth model, Duong model, Yu-Miocevic model and extended exponential decline curve. This paper summarized the origins, derivations and assumptions of these eight models. This paper also presents a comparative study of these models using production data from unconventional gas and oil reservoirs. To facilitate conducting this study, the eight decline curve analysis models were programmed in a software application written in python language. This software application calibrated models' parameters to production data using trust region reflective algorithm. The value of estimated ultimate recovery predicted using this software application is consistent with that predicted using the linear flow analysis model. The comparative study can serve as a guideline for petroleum engineers to determine when to use each model.

Introduction

Petroleum reservoirs are subsurface hydrocarbon-bearing rocks. They are classified as conventional and unconventional reservoirs. Conventional reservoirs are characterized by high permeability while unconventional ones are characterized by very low permeability. Unlike conventional reservoirs, drilling multi-fractured horizontal wells (MFHWs) and multiple horizontal wells from a single pad are considered as parts of well completion operations [1-4]. They enhance well productivity in unconventional reservoirs. As, the horizontal well maximizes the contact area between the wellbore and the reservoir and the fractures work as paths for hydrocarbon to flow toward the wellbore.

Wells producing from unconventional reservoirs have production performance which exhibits long-term transient flow regime followed by boundary-dominated flow (BDF) regime. Transient flow may be linear, bilinear or both according to reservoir and well characteristics. A backflow period occurs ahead of transient flow due to cleaning the well from fracturing fluid when MFHWs are used. Various production data analysis (PDA) methods have been developed to identify these flow regimes, evaluate the reservoir and the well, and predict the well future production performance. Clarkson [5] reviewed five PDA methods that have been commonly applied for unconventional reservoirs including analytical and numerical simulation methods, straight-line analysis methods, type-curve methods, empirical methods, and hybrid methods. Analytical and numerical methods are used to simulate fluid flow in porous medium. Analytical models use solutions to simple reservoir behaviour [6-11] while numerical simulation ones use solutions to more complex reservoir behaviour [12-14]. Straight-line analysis methods are analogous to those used in pressure transient analysis [15]. They are used for flow-regime identification. Araya and Ozkan [16] and Medeiros et al. [17,18] used the transient productivity index as another tool for flow-regime identification. Type-curve methods involve matching of production data to dimensionless solutions to flow equations

[7,8,19,20]. These solutions correspond to different well, fracture and reservoir properties and boundary conditions. Empirical methods are also called decline curve analysis (DCA) methods. They use mathematical models for curve-fit of production data. These models are not necessarily derived from a physical model as with analytical models. Many DCA models have been developed to predict production behaviour in unconventional reservoirs and determine the estimated ultimate recovery (EUR). Kanfar and Wattenbarger [21], Tan et al. [22], Mahmoud et al. [23], Ibrahim et al. [24] and Liang et al. [25] reviewed and evaluated different DCA models. Several studies used machine learning for improving the prediction of production behaviour in unconventional reservoirs and automating the application of some DCA models [26-28]. Hybrid methods are those that involve analytical methods to represent transient flow and empirical methods to represent BDF [29,30]. In this study, we focused on DCA methods as they are considered the most suitable methods for forecasting production behaviour and estimating ultimate recovery in unconventional reservoirs. We reviewed eight DCA models and programmed them in a software application written in python language to facilitate their application. Then, four actual data sets were used to show the more accurate models in simulating and predicting production behaviour of wells in unconventional reservoirs. Finally, conclusions were given for when to use each model, and a recommendation was made.

Modern Decline Curve Analysis Models

Among PDA methods, DCA method is considered the simplest, the least time consumption, and the least data requirement method. Many DCA models have been developed to fit and predict production performance of conventional and unconventional reservoirs. DCA models used for unconventional reservoirs are called modern DCA models to differentiate them from those used for conventional reservoirs [3].

Arps model is considered the most popular and used DCA method in petroleum industry. Arps [31] proposed three different mathematical expressions to simulate production decline-curve behaviour. The author derived these mathematical expressions based on two concepts:

- The loss-ratio definition introduced by Johnson and Bollens [32].
- Production decline curves showed constant loss-ratio and constant derivative of loss-ratio as concluded by Pirson [33].

Where, loss-ratio (1/D) and derivative of loss-ratio (b) have the following mathematical expressions, respectively:

$$\frac{1}{D} = -\frac{q}{\frac{dq}{dt}} \quad (1)$$

$$b = \frac{d}{dt}\left(\frac{1}{D}\right) \quad (2)$$

The mathematical expressions, main characteristics and diagnostic plots of Arps decline curves are shown in Tables 1,2 and Figure 1, respectively.

Table 1 Mathematical expressions of the three types of Arps decline curves

Exponential Decline	Hyperbolic Decline	Harmonic Decline
$b = 0$	$0 < b < 1$	$b = 1$
$D(t) = D_i$ (Eq. (3))	$D(t) = \frac{D_i}{1+b\,D_i\,t}$ (Eq. (4))	$D(t) = \frac{D_i}{1+D_i\,t}$ (Eq. (5))
$q(t) = q_i \exp(-D_i t)$ (Eq. (6))	$q(t) = \frac{q_i}{(1+bD_it)^{\frac{1}{b}}}$ (Eq. (7))	$q(t) = \frac{q_i}{(1+D_it)}$ (Eq. (8))
$Q(t) = \frac{q_i - q(t)}{D_i}$ (Eq. (9))	$Q(t) = \left[\frac{q_i}{D_i(1-b)}\right]\left[1-\left(\frac{q(t)}{q_i}\right)^{1-b}\right]$ (Eq. (10))	$Q(t) = \left(\frac{q_i}{D_i}\right)\ln\left(\frac{q_i}{q(t)}\right)$ (Eq. (11))

Table 2 Main characteristics of the three types of Arps decline-curve diagnostic plots

Plot	Exponential Decline	Hyperbolic Decline	Harmonic Decline
$q\ vs.\ t$ **(Straight Line)**	Semi-Log Plot	Log-Log Plot (Using shifting technique)	Log-Log Plot (Using shifting technique)
$q\ vs.\ Q$ **(Straight Line)**	Coordinate Plot	None	Semi-Log Plot

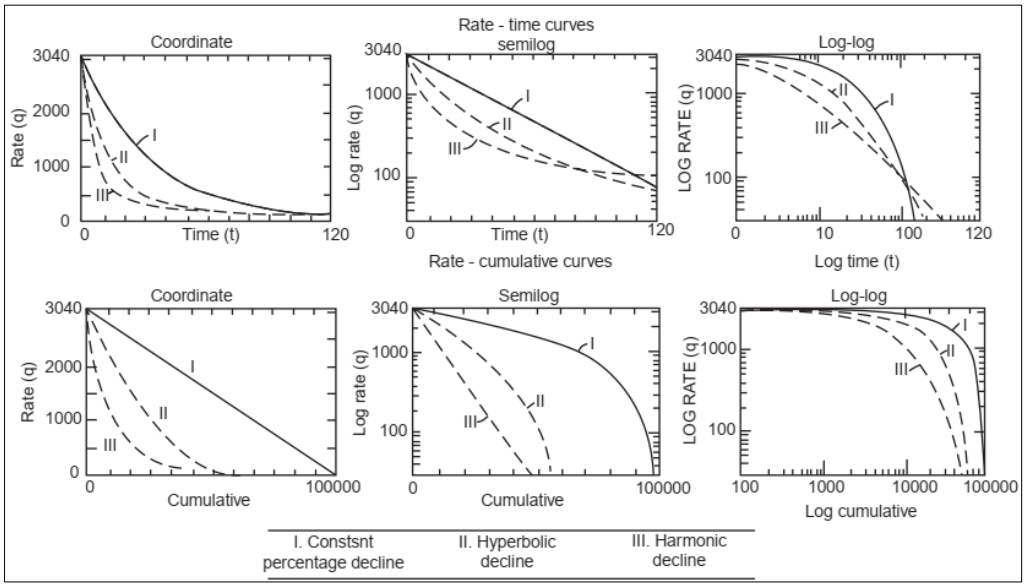

Figure 1 Diagnostic plots of the three types of Arps decline curves (After Arps [34])

Where:

b = Arps decline-curve exponent.
D_i = Initial decline rate, day^{-1}.
$D(t)$ = Decline rate at time t, day^{-1}.
t = Time, day.
q_i = Initial flow rate at time t=0, MSTB/day or MMSCF/day.
$q(t)$ = Flow rate at time t, MSTB/day or MMSCF/day.
$Q(t)$ = Cumulative production, MSTB or MMSCF.
q = Production rate.
Q = Cumulative production.

The limitations of Arps method application are:

- The well produces from a certain area under BDF regime.
- It produces at its capacity and constant bottom-hole flowing pressure.
- There are no changes in well operating conditions.

Wells in unconventional reservoirs violate these limitations as they produce under long-term transient flow regime. So, modern DCA models have been developed to overcome this problem.

Power-Law Exponential (PLE) Model

Ilk et al. [35] proposed an empirical model to fit and predict tight gas and shale production. Their model was derived by integrating an empirical correlation for decline rate (Eq. (12)) which obeys a decaying power-law relation during transient flow regime and a constant relation during BDF regime.

$$D(t) = D_\infty + D_1\, t^{-(1-n)} \quad (12)$$

$$q(t) = \hat{q}_i exp\left[-D_\infty\, t - \hat{D}_i\, t^n\right] \quad (13)$$

Where:

$q(t)$ = Flow rate at time t, MSTB/day or MMSCF/day.
$\hat{q}_i$ = Rate intercept at t = 0 [This parameter has a different interpretation than q_i].
$D(t)$ = Decline rate at time t, day^{-1}.
D_1 = Decline constant intercept at t = 1 day.
D_∞ = Decline constant at infinite time.
$\hat{D}_i$ = Decline constant $[\hat{D}_i = D_1/n]$ [This parameter has a different interpretation than D_i].
t = Time, day.
n = Time exponent.

Stretched Exponential Production Decline (SEPD) Model

Valkó [36] developed an empirical DCA model which is fundamentally different from Arps model. The model is called stretched exponential production decline (SEPD) as production rate obeys a decaying exponential relation as follows:

$$q = q_i\, exp\left[-\left(\frac{t}{\tau}\right)^n\right] \quad (14)$$

Where:

q = Produced rate in period, MSCF/month
q_i = Maximum observed production rate, MSCF/month
t = Number of periods, months
n = Model exponent
τ = characteristic number of periods

This model was developed specifically for the case of even data taken periodically. It is different from power-law exponential model. As it doesn't consider the behaviour of the late-time stage flow regime besides providing a cumulative-time relation (Eq. (15)) which can be used to obtain model's parameters (n and τ) from curve fitting of cumulative production data when production rate data is very scattered.

$$Q = \frac{q_i\,\tau}{n}\left\{\Gamma\left[\frac{1}{n}\right] - \Gamma\left[\frac{1}{n}, \left(\frac{t}{\tau}\right)^n\right]\right\} \quad (15)$$

Where:

Q = Cumulative production, MSCF
$\Gamma\left[\frac{1}{n}\right]$ = Complete gamma function

$\Gamma\left[\frac{1}{n}, \left(\frac{t}{\tau}\right)^n\right]$ = Incomplete gamma function

T-Model

Huang et al. [37] and Hu and Chen [38] had studied huge field production data and deduced that oil cumulative production (N_p) was related to time (t) by the following differential equation which was called T-Model:

$$\frac{dN_p}{N_p\ dt} = a\ t^{\,b} \tag{16}$$

Dou et al. [39] integrated the above equation to obtain cumulative-time relation, which is:

$$N_p = N_R\ e^{\left(\frac{a}{b+1} t^{\,b+1}\right)} \tag{17}$$

The rate-time relation is:

$$q(t) = a\ N_R\ t^{\,b}\ e^{\left(\frac{a}{b+1} t^{\,b+1}\right)} \tag{18}$$

Where:

$q(t)$ = Oil production rate, STB/day
N_p = Cumulative oil production, STB
N_R = Ultimate oil recovery at $t \rightarrow \infty$, STB
t = Producing time, days
a = Model's constant
b = Model's constant

Logistic Growth Model (LGM)

Clark et al. [40] developed the following two relations. They were derived by alternating the logistic growth model that was used by Spencer and Coulombe [41] to predict the production performance of tight and unconventional reservoirs.

LGM cumulative-time relation:

$$Q(t) = \frac{K\ t^{\,n}}{a + t^{\,n}} \tag{19}$$

LGM rate-time relation:

$$q(t) = \frac{K\ n\ a\ t^{\,n-1}}{(a + t^{\,n})^{\,2}} \tag{20}$$

Where:

$Q(t)$ = Cumulative production.
$q(t)$ = Production rate.
K = Carrying capacity or Estimated ultimate recovery
a = Model constant.
n = Hyperbolic exponent.
t = Time.

Duong Model

Duong [42] developed an approach to model production performance of fractured wells producing from super tight and shale reservoirs. This approach accounted for the presence of fracture-dominated flow regimes. It can accurately predict production performance and reserve estimation of those reservoirs.

Duong time/material balance-time relation:

$$\frac{q}{G_P} = a\ t^{\,-1} \tag{21}$$

Duong modified time/material-balance-time relation:

$$\frac{q}{G_P} = a\ t^{\,-m} \tag{22}$$

Duong rate-time relation:

$$\frac{q}{q_1} = t^{\,-m} e^{\frac{a}{1-m}(t^{\,1-m}-1)} \tag{23}$$

Duong cumulative-time relation:

$$G_P = \frac{q_1}{a}\ e^{\frac{a}{1-m}(t^{\,1-m}-1)} \tag{24}$$

Where:

q = Production rate, MMSCF/day.
q_1 = Production rate at t = 1 day , MMSCF/day.
G_P = Cumulative gas production, MMSCF.
t = Time, day.
a = Intercept constant defined by Eq. (22)
m = Slope defined by Eq. (22)

YM-SEPD Model

To overcome the non-uniqueness problem appearing when using non-linear regression to find parameters of SEPD model, Yu and Miocevic [43] introduced a new specialized plot which enabled the calculation of $n\ and\ \tau$ parameters of SEPD model. They proposed the following relation which indicated that plotting $ln(q_i/q(t))$ versus t on a log-log scale produces a straight-line relationship with n as the slope and τ is calculated from the intercept.

$$ln\left(\frac{q_i}{q(t)}\right) = \tau^{-n}\ t^n \tag{25}$$

Extended Exponential Decline Curve (EED)

Zhang et al. [44] developed an empirical equation to determine a-parameter in the equation proposed by Fetkovich [45]. This empirical equation was developed based on the concept of growing drainage volume in shale reservoirs. It could simulate the production behaviour of transient, BDF and transition period between them.

Fetkovich equation:

$$q = q_i\ e^{-a\ t} \tag{26}$$

Where:

q = Flow rate at time t.
q_i = Initial flow rate.
a = Nominal decline rate.

Zhang et al. empirical equation:

$$a = \beta_l + \beta_e\ e^{-\ t^{\,n}} \tag{27}$$

Where:

β_e = Constant to account for the early (fully transient) period, which should be larger than β_l as recommended.
β_l = Constant to account for the late-life (BDF) period.
n = Empirical exponent, with a recommended range of 0 to 0.7
t = Time in months.

Combined Models

Some authors used different type of DCA models which is called combined models. Combined models containing two models, also called dual models, are such as PLE + Arps (modified PLE) [46] and Duong + Arps (modified Duong) [47,48]. The switch point of these models has no physical basis and just assumed based on experience. Chen et al. [49] proposed a combined model by using SEPD, Duong, and Arps. This

model is more complex and has more undetermined coefficients which make it harder to use.

Methodology

DCA models can't be used to predict future production behaviour until they achieve good curve-fit to production data. To automate curve fitting and prediction processes, we programmed DCA models in a software application written in python language which we called production data analysis software (PDAS) application. The PDAS application consists of seven tabs. In this study, we only used three tabs, which are:

- Curve fitting tab: to calibrate parameters of DCA models to production data. It uses the trust region reflective algorithm to calculate parameters' values which achieve the best curve fit. Statistical parameters are also calculated to determine the degree of curve-fit accuracy. Statistical parameters used are coefficient of determination (R^2) and root mean square error ($RMSE$).
- Future prediction tab: to graphically predict the future production behaviour.
- Results tab: to calculate values of time and cumulative production corresponding to production rate at economic limit.

In this study, we ignored combined DCA models and only used the other DCA models (Arps and seven modern DCA models). As combined models aren't basic models in the strict sense, as no new models are created. This paper presents a comparative study to show: Which one of DCA models can fit the production data with the highest accuracy? Is this model can also predict the future production performance or not? Is it necessary to develop a new model to increase the accuracy of curve fitting and future prediction? These questions will be answered in the following sections. The following steps explain how to apply a DCA model using production data of unconventional reservoirs:

1) Using excel sheet, production data is checked to remove very scattered data points. The remaining data is uploaded to the PDAS application to be used in the next steps.
2) In curve fitting tab, parameters of a DCA model are calibrated to the production data. Calibrated parameters are used to check the curve-fit accuracy through determining values of R^2 and $RMSE$. Better accuracy is achieved when R^2 value is close to 1 and $RMSE$ value is low.
3) Future prediction tab is used to plot the production behaviour as predicted using the calibrated DCA model.
4) In results tab, the value of production rate at economic limit is entered then the PDAS application uses the calibrated DCA model to predict producing time and cumulative production corresponding to this value. This cumulative production refers to EUR.

Results and Discussion

A comparison of decline curve analysis models was conducted on how they could fit and predict production performance of wells producing from unconventional reservoirs. Four actual unconventional reservoir data sets were used (2 gas cases and 2 oil cases). Symbols used in this comparison are given in Table 3.

Table 3 Symbols used in the comparison of DCA Models

EUR	Estimated ultimate recovery
G_P	Cumulative gas production
N_P	Cumulative oil production
Q_g	Gas production rate
$Q_{g_{inj}}$	Gas injection rate (Gas Lift)
Q_{limit}	Production rate at economic limit
Q_o	Oil production rate
$RMSE\ (G_P)$	RMSE for cumulative gas production
$RMSE\ (N_P)$	RMSE for cumulative oil production
$RMSE\ (Q_g)$	RMSE for gas production rate
$RMSE\ (Q_o)$	RMSE for oil production rate
$R^2\ (G_P)$	R^2 for cumulative gas production
$R^2\ (N_P)$	R^2 for cumulative oil production
$R^2\ (Q_g)$	R^2 for gas production rate
$R^2\ (Q_o)$	R^2 for oil production rate
t	Producing time
t_{limit}	Time at economic limit

Gas Case 1

The first case is a dataset of a well producing from unconventional dry gas reservoir, summarized by Ahmed [3]. Firstly, we checked the quality of the production data and removed very scattered data. Then, we used the remaining data in the PDAS application for analysis by eight DCA models. Table 4 shows results of model's parameters, coefficient of determination and root mean square error of curve fitting of these eight models.

The results shows that Duong, T and EED models recorded the highest accuracy in fitting production rate data, respectively. R^2 for production curves of Duong and T models are nearly equal. So, these curves can't be distinguished as seen in Figure 2. EED model has the least accuracy among the three models in predicting the future production performance of the well. As rate curve bent away from production data at late-time stage.

All models were extended to reach the economic limit of gas production rate $Q_g = 0.1\ MMSCF/day$. Each model recorded different value of estimated ultimate recovery, see Table 5. According to Mahmoud et al. [23], Duong model overestimated the EUR value which may be three times greater than that predicted using Arps or SEPD models. The authors attributed the reason to the linear flow assumption of Duong model which failed to match the BDF period. They also advised that this assumption will generally need modifications to deal with changes in the flow

regimes. From Figure 2 and Table 5, we found that Duong model matched the BDF period and predicted EUR value of 0.79 MMMSCF, respectively. This EUR value is near those predicted using Arps and SEPD models. The reason is due to the way of calibrating the parameters of Duong model. We calibrated these parameters only to the production data of transient and BDF periods as we removed data of backflow period. However, production data of backflow period was used when statistical parameters were determined to show the accuracy of the model in matching all flow-regime types. The same modification was applied when using T-model to increase its curve-fit accuracy as T and Duong models have similar mathematical expressions.

Table 4 Comparison of curve fitting parameters and statistical values of DCA models for gas case 1

Arps Model			**PLE Model**			**SEPD Model**			**T-Model**		
q_i	=	5.2806	q_i	=	5.2316	q_i	=	6.0000	a	=	4.6717
D_i	=	0.0106	D_1	=	0.0140	τ	=	97.591	b	=	-1.4648
b	=	0.3612	D_∞	=	0.0000	n	=	0.7356	G_R	=	1150.2
			n	=	0.8612						
$R^2\ (Q_g)$	=	0.9197	$R^2\ (Q_g)$	=	0.9119	$R^2\ (Q_g)$	=	0.9052	$R^2\ (Q_g)$	=	0.9514
$RMSE\ (Q_g)$	=	0.3382	$RMSE\ (Q_g)$	=	0.3544	$RMSE\ (Q_g)$	=	0.3675	$RMSE\ (Q_g)$	=	0.2632
$R^2\ (G_P)$	=	0.9970	$R^2\ (G_P)$	=	0.9945	$R^2\ (G_P)$	=	0.9924	$R^2\ (G_P)$	=	0.9949
$RMSE\ (G_P)$	=	8.7177	$RMSE\ (G_P)$	=	11.700	$RMSE\ (G_P)$	=	13.757	$RMSE\ (G_P)$	=	11.267
LGM Model			**Duong Model**			**YM-SEPD Model**			**EED Model**		
a	=	100.00	q_1	=	0.2277	q_i	=	6.0000	q_i	=	5.2258
n	=	0.8294	a	=	4.6717	τ	=	90.806	β_e	=	1.3459
K	=	1078.2	m	=	1.4648	n	=	0.6505	β_l	=	0.0082
									n	=	0.7000
$R^2\ (Q_g)$	=	0.7789	$R^2\ (Q_g)$	=	0.9529	$R^2\ (Q_g)$	=	0.8967	$R^2\ (Q_g)$	=	0.9308
$RMSE\ (Q_g)$	=	0.5614	$RMSE\ (Q_g)$	=	0.2590	$RMSE\ (Q_g)$	=	0.3837	$RMSE\ (Q_g)$	=	0.3139
$R^2\ (G_P)$	=	0.9977	$R^2\ (G_P)$	=	0.9921	$R^2\ (G_P)$	=	0.9964	$R^2\ (G_P)$	=	0.9876
$RMSE\ (G_P)$	=	7.5333	$RMSE\ (G_P)$	=	14.054	$RMSE\ (G_P)$	=	9.4379	$RMSE\ (G_P)$	=	17.606

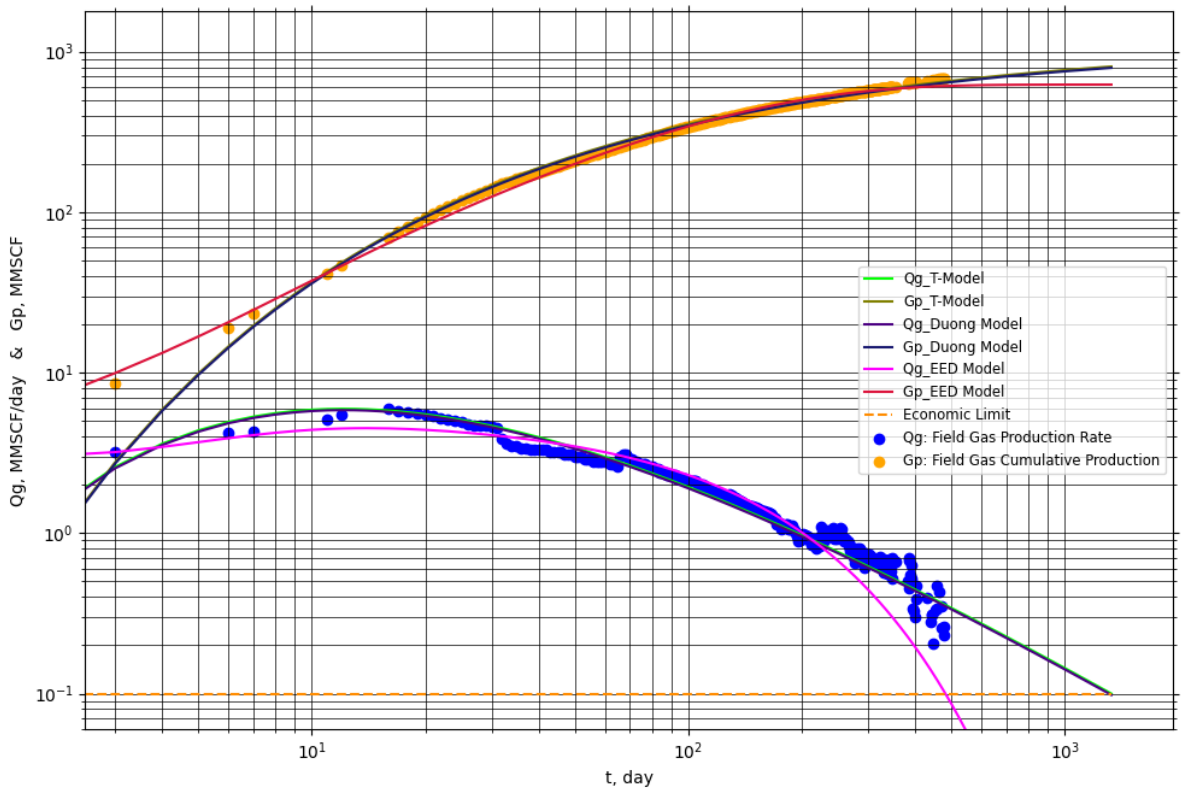

Figure 2 Comparison of future prediction of Duong, T and EED models for gas case 1

Table 5 Comparison of estimated ulimate recovery of DCA models for gas case 1

Arps Model			**PLE Model**			**SEPD Model**			**T-Model**		
$Q_{limit}, \frac{MMSCF}{day}$	=	0.10	$Q_{limit}, \frac{MMSCF}{day}$	=	0.10	$Q_{limit}, \frac{MMSCF}{day}$	=	0.10	$Q_{limit}, \frac{MMSCF}{day}$	=	0.10
t_{limit}, day	=	834	t_{limit}, day	=	590	t_{limit}, day	=	663	t_{limit}, day	=	1331
EUR, MMMSCF	=	0.72	EUR, MMMSCF	=	0.66	EUR, MMMSCF	=	0.68	EUR, MMMSCF	=	0.81
LGM Model			**Duong Model**			**YM-SEPD Model**			**EED Model**		
$Q_{limit}, \frac{MMSCF}{day}$	=	0.10	$Q_{limit}, \frac{MMSCF}{day}$	=	0.10	$Q_{limit}, \frac{MMSCF}{day}$	=	0.10	$Q_{limit}, \frac{MMSCF}{day}$	=	0.10
t_{limit}, day	=	1411	t_{limit}, day	=	1312	t_{limit}, day	=	793	t_{limit}, day	=	482
EUR, MMMSCF	=	0.87	EUR, MMMSCF	=	0.79	EUR, MMMSCF	=	0.71	EUR, MMMSCF	=	0.61

Gas Case 2

The second case is a dataset of well # 314 producing from Barnett shale as shown in Figure 3. The decline curve shows that a backflow period occurred ahead of transient flow due to cleaning the well from fracturing fluid. The properties of the reservoir and the well are given in Table 6. Al-Ahmadi et al. [50] studied this data and used it as an example to display the application procedures of linear flow analysis to shale gas wells. We used this data in the PDAS application to show which DCA model could fit it with high accuracy. PLE, Duong and T models, respectively, showed the highest fitting accuracy, as concluded from results in Table 7. The prediction of future production behaviour using these models is shown in Figure 4. The results proved that PLE model predicted the future production behaviour better than other models as PLE production curves passed through production data of late-time stage. EUR value predicted using PLE is equal to 2.67 MMMSCF, as given in Table 8, which is consistent with that calculated by Al-Ahmadi et al. [50] (2.74 MMMSCF) when using the linear flow analysis [51]. Also, EUR values predicted using the other DCA models are near that value, and this proved that the PDAS application is a powerful and reliable tool that can be used for production data analysis of unconventional reservoirs.

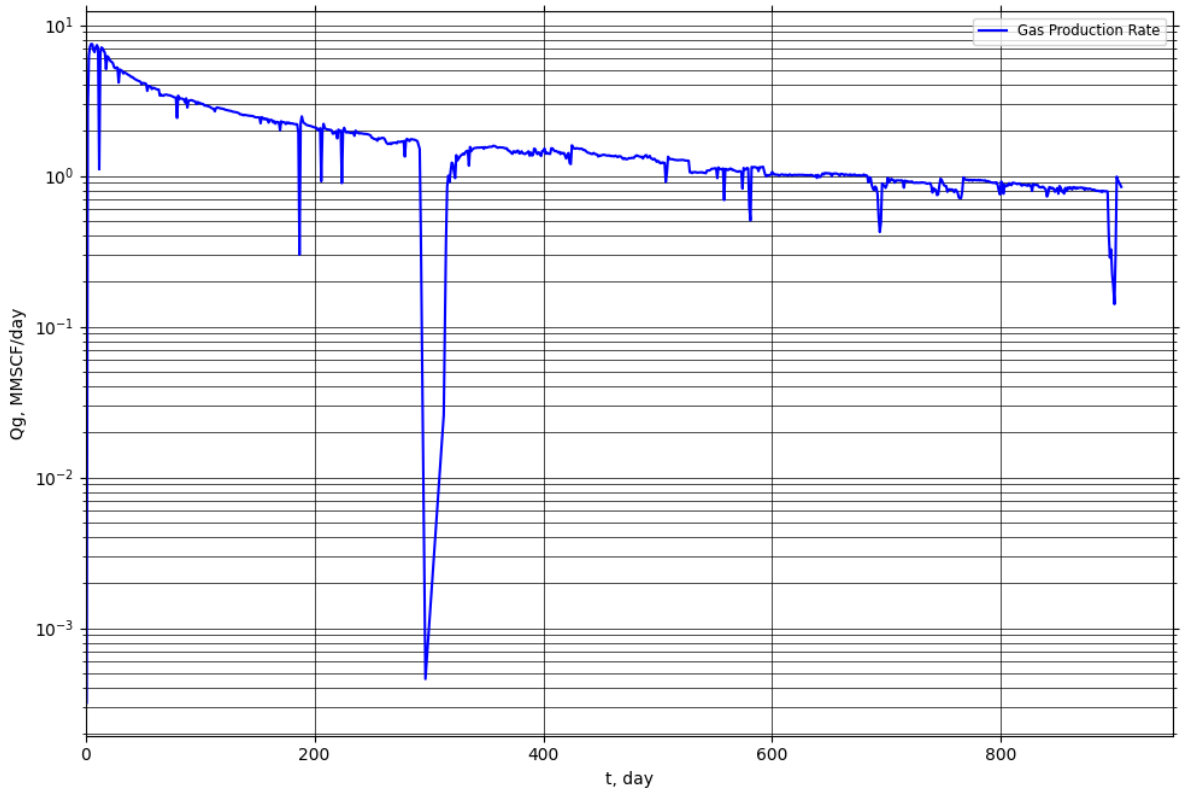

Figure 3 Production decline curve for gas case 2

Table 6 Reservoir, fluid and well data for gas case 2

Porosity, Ø (fraction)	0.06	Initial gas formation volume factor, β_{gi} (ft^3/SCF)	0.00509
Gas viscosity at initial reservoir pressure, μ_{gi} (cp)	0.0201	Real gas pseudo − pressure at initial reservoir pressure, $m(P_i)$ (psi^2/cp)	$5.97 * 10^8$
Total copressibility coefficient at initial reservoir pressure, C_{ti} (psi^{-1})	$220 * 10^{-6}$	Real gas pseudo − pressure at bottom − hole flowing pressure, (P_{wf}) (psi^2/cp)	$2.03 * 10^7$
Initial gas saturation, S_{gi}	0.70	Number of perforation clusters, n_f	28
Reservoir temperature, T (°R)	610	Reservoir thickness, h (ft)	300
Assumed matrix permeability, K_m (md)	$1.50 * 10^{-4}$	Drainage area (well) length, x_e (ft)	2968

Table 7 Comparison of curve fitting parameters and statistical values of DCA models for gas case 2

Arps Model		**PLE Model**		**SEPD Model**		**T-Model**	
q_i	= 6.7696	q_i	= 24.186	q_i	= 7.5057	a	= 1.2821
D_i	= 0.0106	D_1	= 0.1654	τ	= 139.38	b	= -1.1413
b	= 1.0000	D_∞	= 0.0000	n	= 0.4831	G_R	= 50873
		n	= 0.2303				
$R^2\ (Q_g)$	= 0.9706	$R^2\ (Q_g)$	= 0.9945	$R^2\ (Q_g)$	= 0.9614	$R^2\ (Q_g)$	= 0.9923
$RMSE\ (Q_g)$	= 0.2008	$RMSE\ (Q_g)$	= 0.0865	$RMSE\ (Q_g)$	= 0.2300	$RMSE\ (Q_g)$	= 0.1028
$R^2\ (G_P)$	= 0.9949	$R^2\ (G_P)$	= 0.9984	$R^2\ (G_P)$	= 0.9981	$R^2\ (G_P)$	= 0.9993
$RMSE\ (G_P)$	= 29.242	$RMSE\ (G_P)$	= 16.522	$RMSE\ (G_P)$	= 17.761	$RMSE\ (G_P)$	= 10.885
LGM Model		**Duong Model**		**YM-SEPD Model**		**EED Model**	
a	= 100.00	q_1	= 7.5428	q_i	= 7.5057	q_i	= 4.4984
n	= 0.6245	a	= 1.2821	τ	= 120.43	β_e	= 1.0000
K	= 3636.4	m	= 1.1413	n	= 0.4134	β_l	= 0.0028
						n	= 0.7000
$R^2\ (Q_g)$	= 0.9358	$R^2\ (Q_g)$	= 0.9926	$R^2\ (Q_g)$	= 0.9446	$R^2\ (Q_g)$	= 0.8127
$RMSE\ (Q_g)$	= 0.2964	$RMSE\ (Q_g)$	= 0.1009	$RMSE\ (Q_g)$	= 0.2754	$RMSE\ (Q_g)$	= 0.5065
$R^2\ (G_P)$	= 0.9820	$R^2\ (G_P)$	= 0.9986	$R^2\ (G_P)$	= 0.9875	$R^2\ (G_P)$	= 0.9874
$RMSE\ (G_P)$	= 55.134	$RMSE\ (G_P)$	= 15.322	$RMSE\ (G_P)$	= 45.889	$RMSE\ (G_P)$	= 46.203

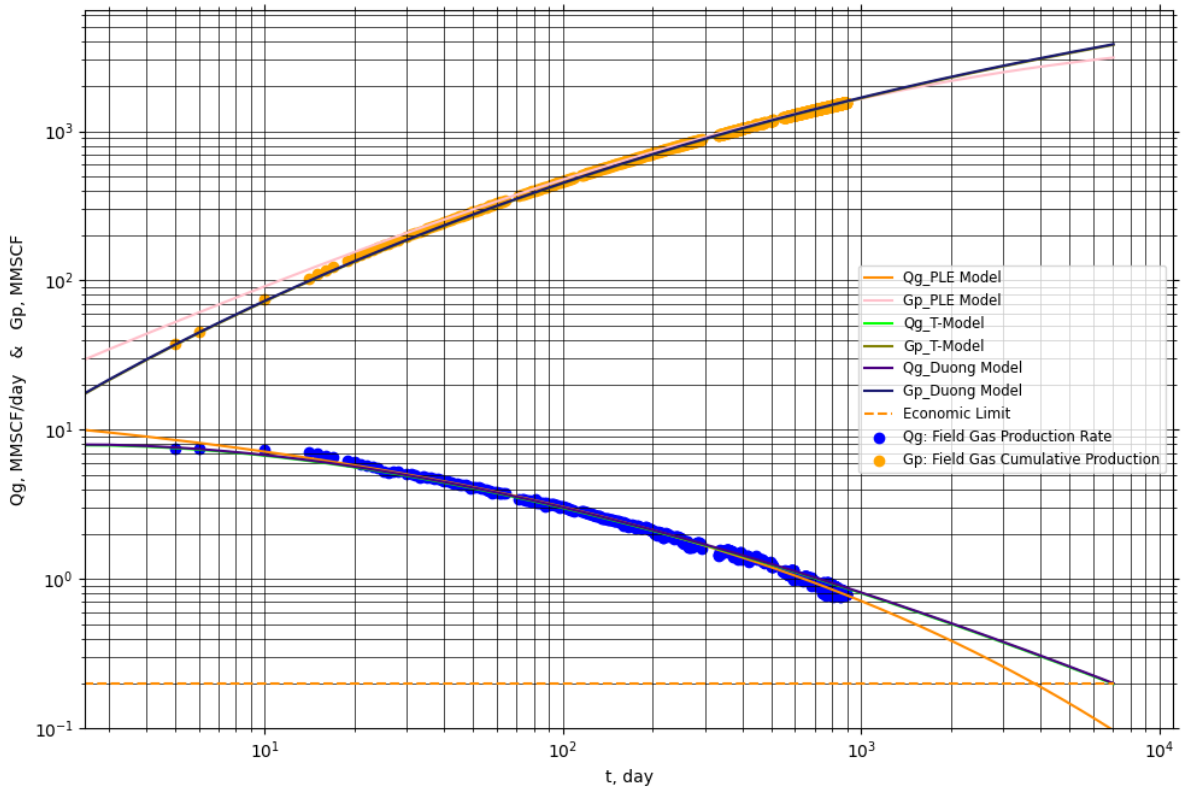

Figure 4 Comparison of future prediction of PLE, Duong and T models for gas case 2

Table 8 Comparison of estimated ulimate recovery of DCA for gas case 2

Arps Model	PLE Model	SEPD Model	T-Model
$Q_{limit}, \frac{MMSCF}{day} = 0.200$	$Q_{limit}, \frac{MMSCF}{day} = 0.200$	$Q_{limit}, \frac{MMSCF}{day} = 0.200$	$Q_{limit}, \frac{MMSCF}{day} = 0.200$
$t_{limit}, day = 3088$	$t_{limit}, day = 3807$	$t_{limit}, day = 2005$	$t_{limit}, day = 6936$
$EUR, MMMSCF = 2.241$	$EUR, MMMSCF = 2.670$	$EUR, MMMSCF = 1.937$	$EUR, MMMSCF = 3.775$
LGM Model	**Duong Model**	**YM-SEPD Model**	**EED Model**
$Q_{limit}, \frac{MMSCF}{day} = 0.200$	$Q_{limit}, \frac{MMSCF}{day} = 0.200$	$Q_{limit}, \frac{MMSCF}{day} = 0.200$	$Q_{limit}, \frac{MMSCF}{day} = 0.200$
$t_{limit}, day = 2757$	$t_{limit}, day = 7023$	$t_{limit}, day = 2714$	$t_{limit}, day = 1122$
$EUR, MMMSCF = 2.126$	$EUR, MMMSCF = 3.829$	$EUR, MMMSCF = 2.231$	$EUR, MMMSCF = 1.539$

Oil Case 1

An example of oil production data is that of well # 1 producing from Eagle Ford formation [52]. As well # 1 was completed by 28 stages of hydraulic fracturing, its production history, shown in Figure 5, included a backflow period which lasted for few days. The curve fitting and future prediction processes for production behaviour of this well proved that:

i. PLE, Duong, T and Arps models fitted the production data very well, as demonstrated in Table 9.

ii. These four models predicted the future production performance nearly with the same behaviour as shown in Figure 6 and concluded from EUR values summarized in Table 10.

iii. Although, Arps model was developed to fit production performance of conventional reservoirs [24,31], it fitted production data of well # 1 with high accuracy. The reason is because transient flow regime period didn't last for long time and most of the production data was in BDF regime period.

Oil Case 2

Another example of oil production data is that of Well # 7 producing from Eagle ford formation in Sparrow field [52]. Well # 7 was completed with 49 stages of hydraulic fracturing. The well experienced a decline in production curve before applying the gas lift technique, as shown in Figure 7.

Statistical values summarized in Table 11 proved that EED, Arps, PLE and SEPD models were the most accurate models in fitting production data of Well # 7. These models predicted future production very well and Arps model showed the best prediction as demonstrated in Figure 8. Again, EED model showed the least prediction as with gas case 1. Estimated ultimate recovery values calculated using the eight DCA models are summarized in Table 12. They were calculated when oil rate was 10 STB/day which we assumed as the economic limit for this well.

Due to the long backflow and BDF periods, T and Duong models showed very low accuracy in fitting the production data of well # 7. This is because they were originally developed to model long-term transient flow regime [39,42].

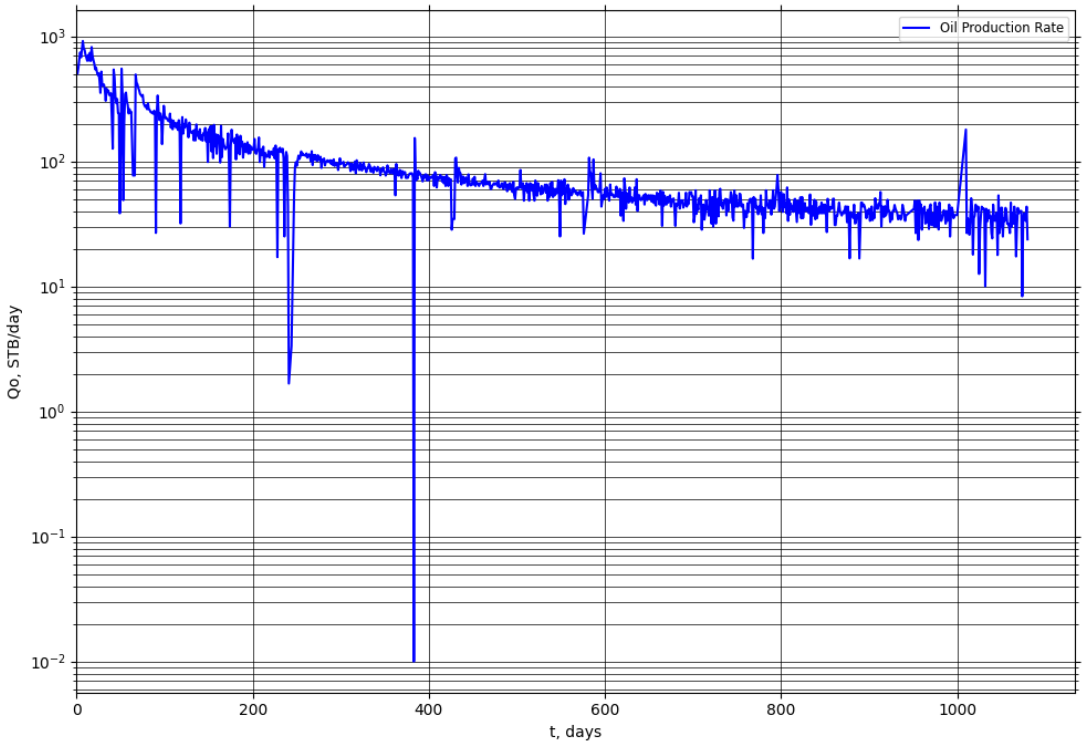

Figure 5 Production decline curve for oil case 1

Table 9 Comparison of curve fitting parameters and statistical values of DCA models for oil case 1

Arps Model		PLE Model		SEPD Model		T-Model	
q_i	= 935.63	q_i	= 9776.3	q_i	= 915.05	a	= 1.6799
D_i	= 0.0319	D_1	= 0.2978	τ	= 55.489	b	= -1.2545
b	= 1.0000	D_∞	= 0.0000	n	= 0.4690	N_R	= 3.2*10^5
		n	= 0.1713				
$R^2\ (Q_o)$	= 0.9716	$R^2\ (Q_o)$	= 0.9805	$R^2\ (Q_o)$	= 0.9294	$R^2\ (Q_o)$	= 0.9769
$RMSE\ (Q_o)$	= 17.343	$RMSE\ (Q_o)$	= 14.394	$RMSE\ (Q_o)$	= 27.355	$RMSE\ (Q_o)$	= 15.651
$R^2\ (N_P)$	= 0.9926	$R^2\ (N_P)$	= 0.9696	$R^2\ (N_P)$	= 0.9862	$R^2\ (N_P)$	= 0.9956
$RMSE\ (N_P)$	= 1956.2	$RMSE\ (N_P)$	= 3973.2	$RMSE\ (N_P)$	= 2672.3	$RMSE\ (N_P)$	= 1509.0
LGM Model		**Duong Model**		**YM-SEPD Model**		**EED Model**	
a	= 81.922	q_1	= 722.56	q_i	= 915.05	q_i	= 554.77
n	= 0.6398	a	= 1.6799	τ	= 27.754	β_e	= 1.0000
K	= 2.1*10^5	m	= 1.2545	n	= 0.3337	β_l	= 0.0067
						n	= 0.7000
$R^2\ (Q_o)$	= 0.9631	$R^2\ (Q_o)$	= 0.9774	$R^2\ (Q_o)$	= 0.8528	$R^2\ (Q_o)$	= 0.7540
$RMSE\ (Q_o)$	= 19.767	$RMSE\ (Q_o)$	= 15.466	$RMSE\ (Q_o)$	= 39.498	$RMSE\ (Q_o)$	= 51.063
$R^2\ (N_P)$	= 0.9997	$R^2\ (N_P)$	= 0.9917	$R^2\ (N_P)$	= 0.8735	$R^2\ (N_P)$	= 0.7095
$RMSE\ (N_P)$	= 423.32	$RMSE\ (N_P)$	= 2073.9	$RMSE\ (N_P)$	= 8105.0	$RMSE\ (N_P)$	= 12280

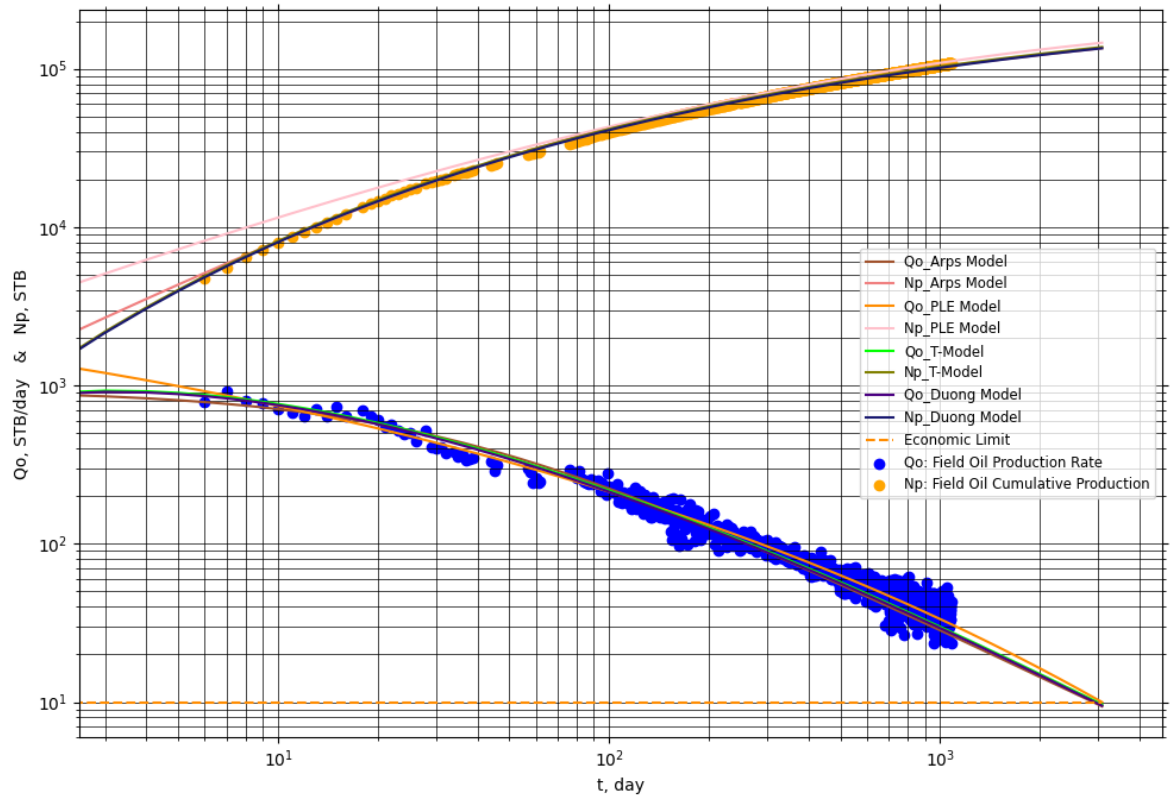

Figure 6 Comparison of future prediction of PLE, Duong, T and Arps models for oil case 1

Table 10 Comparison of estimated ulimate recovery of DCA models for oil case 1

Arps Model		PLE Model		SEPD Model		T-Model	
$Q_{limit}, \frac{MSTB}{day}$	= 0.010	$Q_{limit}, \frac{MSTB}{day}$	= 0.010	$Q_{limit}, \frac{MSTB}{day}$	= 0.010	$Q_{limit}, \frac{MSTB}{day}$	= 0.010
t_{limit}, day	= 2902	t_{limit}, day	= 3086	t_{limit}, day	= 1381	t_{limit}, day	= 2985
EUR, MMSTB	= 0.133	EUR, MMSTB	= 0.146	EUR, MMSTB	= 0.107	EUR, MMSTB	= 0.136
LGM Model		**Duong Model**		**YM-SEPD Model**		**EED Model**	
$Q_{limit}, \frac{MSTB}{day}$	= 0.010	$Q_{limit}, \frac{MSTB}{day}$	= 0.010	$Q_{limit}, \frac{MSTB}{day}$	= 0.010	$Q_{limit}, \frac{MSTB}{day}$	= 0.010
t_{limit}, day	= 2953	t_{limit}, day	= 2936	t_{limit}, day	= 2544	t_{limit}, day	= 603
EUR, MMSTB	= 0.140	EUR, MMSTB	= 0.133	EUR, MMSTB	= 0.126	EUR, MMSTB	= 0.081

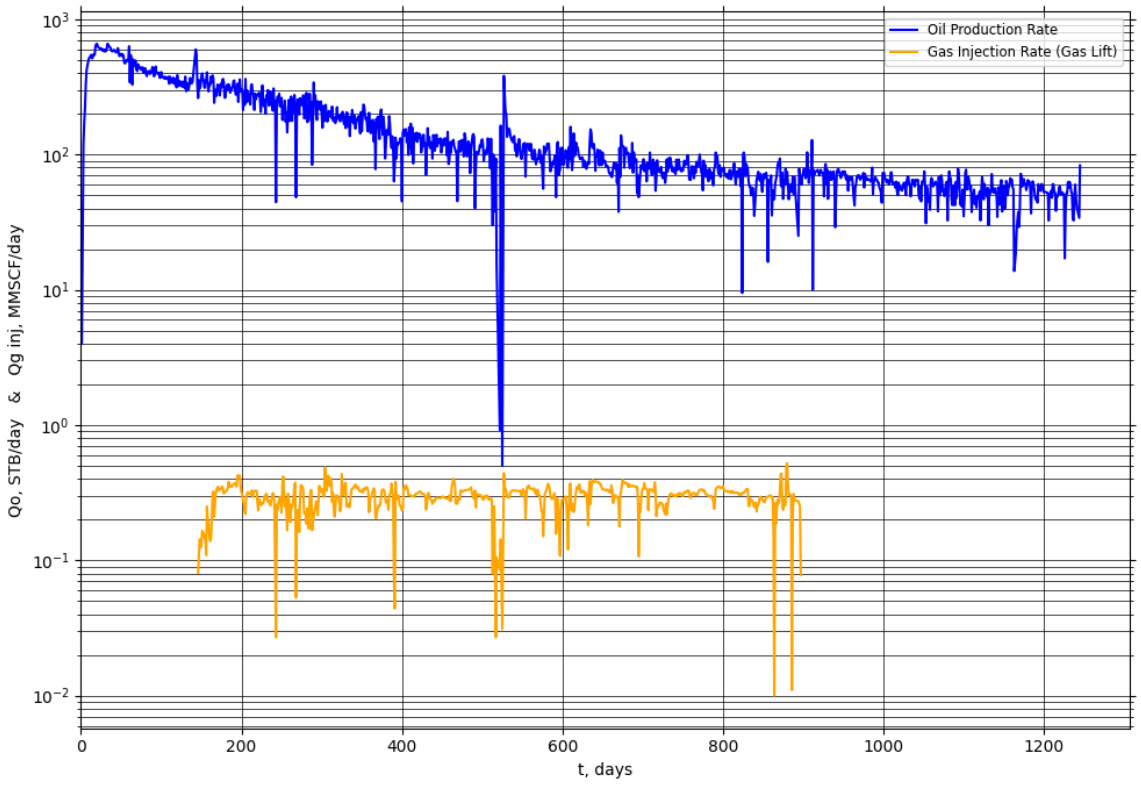

Figure 7 Production decline curve and gas injection rate for oil case 2

Table 11 Comparison of curve fitting parameters and statistical values of DCA models for oil case 2

Arps Model			**PLE Model**			**SEPD Model**			**T-Model**		
q_i	=	570.07	q_i	=	572.35	q_i	=	659.00	a	=	6.5785
D_i	=	0.0042	D_1	=	0.0077	τ	=	249.04	b	=	-1.5086
b	=	0.4349	D_∞	=	0.0000	n	=	0.6891	N_R	=	2.4*10^5
			n	=	0.8095						
$R^2\ (Q_o)$	=	0.9008	$R^2\ (Q_o)$	=	0.8901	$R^2\ (Q_o)$	=	0.8830	$R^2\ (Q_o)$	=	0.5887
$RMSE\ (Q_o)$	=	42.130	$RMSE\ (Q_o)$	=	44.345	$RMSE\ (Q_o)$	=	45.766	$RMSE\ (Q_o)$	=	85.798
$R^2\ (N_P)$	=	0.9983	$R^2\ (N_P)$	=	0.9965	$R^2\ (N_P)$	=	0.9949	$R^2\ (N_P)$	=	0.9355
$RMSE\ (N_P)$	=	2006.3	$RMSE\ (N_P)$	=	2838.4	$RMSE\ (N_P)$	=	3434.5	$RMSE\ (N_P)$	=	12252
LGM Model			**Duong Model**			**YM-SEPD Model**			**EED Model**		
a	=	99.986	q_1	=	3.0505	q_i	=	659.00	q_i	=	561.03
n	=	0.6785	a	=	6.5785	τ	=	205.86	β_e	=	3.4599
K	=	3.3*10^5	m	=	1.5086	n	=	0.5552	β_l	=	0.0030
									n	=	0.7000
$R^2\ (Q_o)$	=	0.1904	$R^2\ (Q_o)$	=	0.7427	$R^2\ (Q_o)$	=	0.8575	$R^2\ (Q_o)$	=	0.9240
$RMSE\ (Q_o)$	=	120.38	$RMSE\ (Q_o)$	=	67.867	$RMSE\ (Q_o)$	=	50.497	$RMSE\ (Q_o)$	=	36.878
$R^2\ (N_P)$	=	0.9857	$R^2\ (N_P)$	=	0.5429	$R^2\ (N_P)$	=	0.9696	$R^2\ (N_P)$	=	0.9901
$RMSE\ (N_P)$	=	5774.2	$RMSE\ (N_P)$	=	32625	$RMSE\ (N_P)$	=	8407.8	$RMSE\ (N_P)$	=	4796.1

Table 12 Comparison of estimated ultimate recovery of DCA models for oil case 2

Arps Model			**PLE Model**			**SEPD Model**			**T-Model**		
$Q_{limit}, \frac{MSTB}{day}$	=	0.010	$Q_{limit}, \frac{MSTB}{day}$	=	0.010	$Q_{limit}, \frac{MSTB}{day}$	=	0.010	$Q_{limit}, \frac{MSTB}{day}$	=	0.010
t_{limit}, day	=	2633	t_{limit}, day	=	1754	t_{limit}, day	=	1990	t_{limit}, day	=	2400
EUR, MMSTB	=	0.216	EUR, MMSTB	=	0.195	EUR, MMSTB	=	0.203	EUR, MMSTB	=	0.191
LGM Model			**Duong Model**			**YM-SEPD Model**			**EED Model**		
$Q_{limit}, \frac{MSTB}{day}$	=	0.010	$Q_{limit}, \frac{MSTB}{day}$	=	0.010	$Q_{limit}, \frac{MSTB}{day}$	=	0.010	$Q_{limit}, \frac{MSTB}{day}$	=	0.010
t_{limit}, day	=	4306	t_{limit}, day	=	2015	t_{limit}, day	=	2715	t_{limit}, day	=	1332
EUR, MMSTB	=	0.249	EUR, MMSTB	=	0.147	EUR, MMSTB	=	0.214	EUR, MMSTB	=	0.179

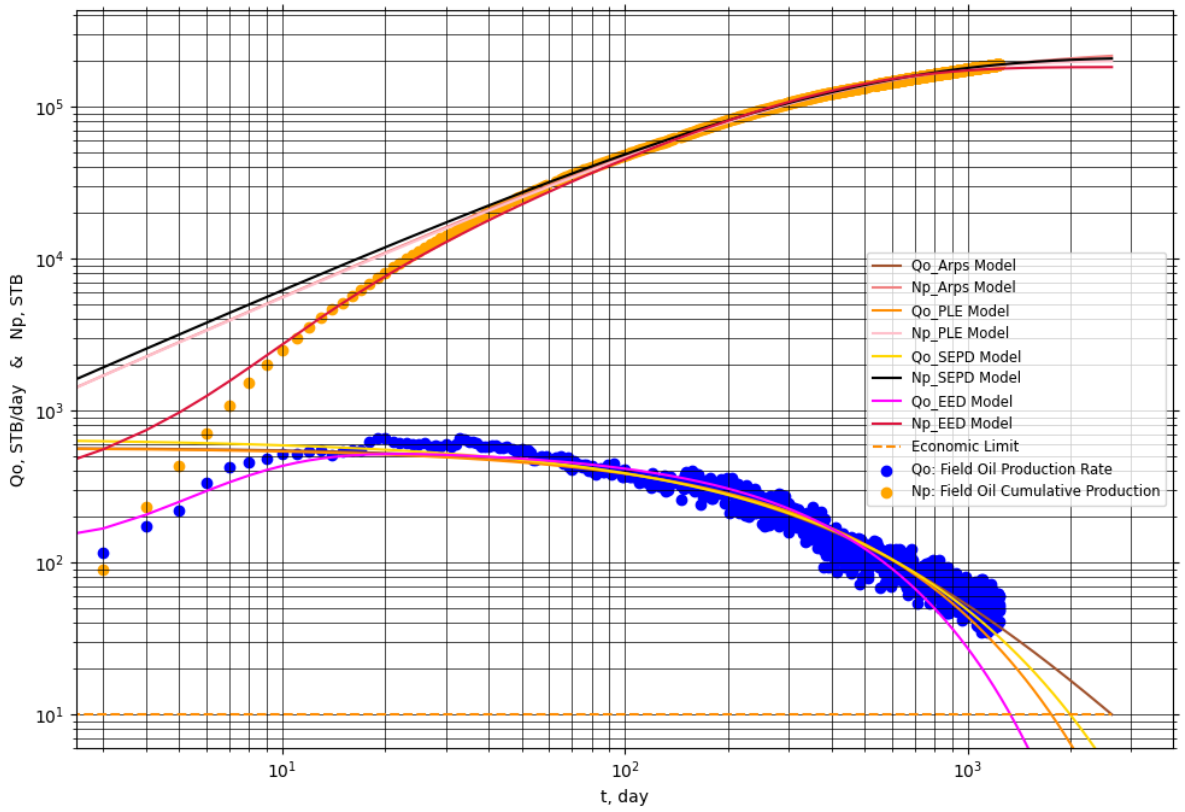

Figure 8 Comparison of future prediction of EED, Arps, PLE and SEPD models for oil case 2

Conclusions

Production behaviour of unconventional reservoirs shows long-term transient flow followed by BDF which required decline curve analysis models other than Arps model. Modern DCA models have been developed to simulate this behaviour, such as PLE, SEPD, T, LGM, Duong, YM-SEPD and EED models. These models along with Arps model were programmed in the PDAS application to facilitate their usage in matching and predicting production behaviour of unconventional reservoirs. Conclusions emanating from the comparative study of these models are as follows:

1) PLE, T and Duong models can simulate production behaviour of wells in unconventional reservoirs with high accuracy.
2) T and Duong models can be used interchangeably as they have similar mathematical expressions and behave with the same manner.
3) The modification used when calibrating the parameters of T and Duong models works well if backflow period is short.
4) Arps model can only fit production data with high accuracy when most of the data is in BDF regime period. It is also considered the most accurate model to represent this flow-regime type.
5) Unlike other models, PLE and EED models consist of two segments: one can simulate early-time stage flow period and the other simulates late-time stage flow period. PLE model can be used to fit and predict production behaviour in unconventional reservoirs while EED model can only be used to fit that behaviour.
6) SEPD model shows moderate accuracy in fitting different flow-regime types simultaneously, as it was originally developed to represent the long-term transient flow. Also, YM-SEPD model shows similar accuracy.
7) Although LGM rate-time relation shows low curve-fit accuracy, the cumulative-time one shows high accuracy. As these relations were adopted from a logistic growth model which basically represented size not rate.
8) The PDAS application is a powerful tool as it minimizes computation time of decline curve analysis. It also provides reliable EUR values compared to those calculated using the linear flow analysis model.

We recommend developing a combined model which consists of two different models (dual model), one can simulate transient flow period plus its preceding backflow period and the other can simulate BDF period. The determination of the switch point should be on a physical basis which enables smooth transformation between the two models. Then, the developed model will be able to simulate the whole production history of wells in unconventional reservoirs and predict their future production behaviour with very high accuracy.

Funding sources

This research received no external funding.

Conflicts of interest

There are no conflicts to declare.

Nomenclature

Abbreviations:

BDF	=	Boundary-dominated flow
DCA	=	Decline curve analysis
EED	=	Extended exponential decline
EUR	=	Estimated ultimate recovery
LGM	=	Logistic growth model
MFHWs	=	Multi-fractured horizontal wells
PDA	=	Production data analysis
PLE	=	Power-law exponential
SEPD	=	Stretched exponential production decline
YM-SEPD	=	Yu and Miocevic - Stretched exponential production decline

Field Variables:

a	=	Model's constant, Intercept constant defined by Eq. (22) or Nominal decline rate
b	=	Derivative of loss ratio, Arps decline-curve exponent or Model's constant
C_{ti}	=	Total compressibility coefficient at initial reservoir pressure, psi^{-1}
D_i	=	Initial decline rate, day^{-1}.
$\widehat{D}_i$	=	Decline constant $[\widehat{D}_i = D_1/n]$ [This parameter has a different interpretation than D_i].
$D(t)$	=	Decline rate at time t, day^{-1}.
D_1	=	Decline constant intercept at t = 1 day.
D_∞	=	Decline constant at infinite time.
$1/D$	=	The loss ratio, time unit.
G_P	=	Cumulative gas production, MMSCF.
h	=	Reservoir thickness, (ft)
K	=	Carrying capacity or estimated ultimate recovery
K_m	=	Assumed matrix permeability, md
m	=	Slope defined by Eq. (22)
$m(P_i)$	=	Real gas pseudo-pressure at initial reservoir pressure, psi^2/cp
$m(P_{wf})$	=	Real gas pseudo-pressure at bottom-hole flowing pressure, psi^2/cp
n	=	Time exponent, Model exponent, Hyperbolic exponent or Empirical exponent, with a recommended range of 0 to 0.7
n_f	=	Number of perforation clusters
N_p	=	Cumulative oil production, STB
N_R	=	Ultimate oil recovery at $t \to \infty$, STB
q	=	Produced rate in period, MSCF/month or Production rate, $MMSCF/day$
q_i	=	Initial flow rate at time t=0, MSTB/day or MMSCF/day or Maximum observed production rate, MSCF/month
$\hat{q}_i$	=	Rate intercept at t = 0 [This parameter has a different interpretation than q_i].
$q(t)$	=	Flow rate at time t, STB/day, MSTB/day or MMSCF/day.
q_1	=	Production rate at $t = 1$ day , $MMSCF/day$.
Q	=	Cumulative production, MSCF
Q_g	=	Gas production rate, MMSCF/day
$Q_{g_{inj}}$	=	Gas injection rate, MMSCF/day
Q_o	=	Oil production rate, STB/day
Q_{limit}	=	Production rate at economic limit, MMSCF/day or MSTB/day
$Q(t)$	=	Cumulative production, MSTB or MMSCF.
$RMSE\ (G_p)$	=	Root mean square error for cumulative gas production.
$RMSE\ (N_p)$	=	Root mean square error for cumulative oil production.
$RMSE\ (Q_g)$	=	Root mean square error for gas production rate.
$RMSE\ (Q_o)$	=	Root mean square error for oil production rate.
$R^2\ (G_p)$	=	Coefficient of determination for cumulative gas production.
$R^2\ (N_p)$	=	Coefficient of determination for cumulative oil production.
$R^2\ (Q_g)$	=	Coefficient of determination for gas production rate.
$R^2\ (Q_o)$	=	Coefficient of determination for oil production rate.
S_{gi}	=	Initial water saturation, fraction
t	=	Time, day or Number of periods, months
t_{limit}	=	Producing time at economic limit, day
T	=	Reservoir temperature, °R
x_e	=	Drainage area (well) length, (ft)

Greek variables:

β_e	=	Constant to account for the early (fully transient) period, which should be larger than β_l as recommended.
β_{gi}	=	Gas formation volume factor at initial reservoir pressure, ft^3/SCF
β_l	=	Constant to account for the late-life (BDF) period.
τ	=	Characteristic number of periods
$\emptyset$	=	Porosity, fraction
μ_{gi}	=	Gas viscosity at initial reservoir pressure, cp
$\Gamma\left[\frac{1}{n}\right]$	=	Complete gamma function
$\Gamma\left[\frac{1}{n}, \left(\frac{t}{\tau}\right)^n\right]$	=	Incomplete gamma function

References

[1] R. Zhang, L. Zhang, R. Wang, Y. Zhao, R. Huang, Simulation of a Multistage Fractured Horizontal Well with Finite Conductivity in Composite Shale Gas Reservoir through Finite-Element Method, *Energy & Fuels*, 30 (11) (2016) 9036–9049. https://doi.org/10.1021/acs.energyfuels.6b01565.

[2] L. Ren, R. Lin, J. Zhao, V. Rasouli, J. Zhao, H. Yang, Stimulated Reservoir Volume Estimation for Shale Gas Fracturing: Mechanism and Modelling Approach, *J. Pet. Sci. Eng.*, 166 (2018) 290–304. https://doi.org/10.1016/j.petrol.2018.03.041.

[3] T. Ahmed, Modern Decline Curve Analysis, in *Reservoir Engineering Handbook*, fifth ed., Gulf Professional Publishing, 2019, pp. 1389–1461. https://doi.org/10.1016/B978-0-12-813649-2.00018-9.

[4] W. Wang, D. Fan, G. Sheng, Z. Chen, Y. Su, A review of analytical and semi-analytical fluid flow models for

ultra-tight hydrocarbon reservoirs, *Fuel*, 256 (2019) 115737. https://doi.org/10.1016/j.fuel.2019.115737.

[5] C.R. Clarkson, Production data analysis of unconventional gas wells: Review of theory and best practices, *Int. J. Coal Geol.*, 109–110 (2013) 101–146. https://doi.org/10.1016/j.coal.2013.01.002.

[6] A.H. El-Banbi, R.A. Wattenbarger, Analysis of Linear Flow in Gas Well Production, in Paper presented at the SPE Gas Technology Symposium, Calgary, Alberta, Canada, March 1998. https://doi.org/10.2118/39972-MS.

[7] R.A. Wattenbarger, A.H. El-Banbi, M.E. Villegas, J.B. Maggard, Production Analysis of Linear Flow Into Fractured Tight Gas Wells, in Paper presented at the SPE Rocky Mountain Regional/Low-Permeability Reservoirs Symposium, Denver, Colorado, April 1998. https://doi.org/10.2118/39931-MS.

[8] R.O. Bello, R.A. Wattenbarger, Rate Transient Analysis in Naturally Fractured Shale Gas Reservoirs, in Paper presented at the CIPC/SPE Gas Technology Symposium 2008 Joint Conference, Calgary, Alberta, Canada, June 2008. https://doi.org/10.2118/114591-MS.

[9] Y. Zhao, L. Zhang, Y. Xiong, Y. Zhou, Q. Liu, D. Chen, Pressure response and production performance for multi-fractured horizontal wells with complex seepage mechanism in box-shaped shale gas reservoir, *J. Nat. Gas Sci. Eng.*, 32 (2016) 66–80. https://doi.org/10.1016/j.jngse.2016.04.037.

[10] S. Huang, G. Ding, Y. Wu, H. Huang, X. Lan, J. Zhang, A semi-analytical model to evaluate productivity of shale gas wells with complex fracture networks, *J. Nat. Gas Sci. Eng.*, 50 (2018) 374–383. https://doi.org/10.1016/j.jngse.2017.09.010.

[11] J. Zeng, W. Li, J. Liu, Y. Leong, D. Elsworth, J. Tian, J. Guo, F. Zeng, Analytical solutions for multi-stage fractured shale gas reservoirs with damaged fractures and stimulated reservoir volumes, *J. Pet. Sci. Eng.*, 187 (2020) 106686. https://doi.org/10.1016/j.petrol.2019.106686.

[12] B. Kulga, T. Ertekin, Numerical representation of multi-component gas flow in stimulated shale reservoirs, *J. Nat. Gas Sci. Eng.*, 56 (2018) 579–592. https://doi.org/10.1016/j.jngse.2018.06.023.

[13] R. Zhang, L. Zhang, H. Tang, S. Chen, Y. Zhao, J. Wu, K. Wang, A simulator for production prediction of multistage fractured horizontal well in shale gas reservoir considering complex fracture geometry, *J. Nat. Gas Sci. Eng.*, 67 (2019) 14–29. https://doi.org/10.1016/j.jngse.2019.04.011.

[14] X. You, J. Liu, C. Jia, J. Li, X. Liao, A. Zheng, Production data analysis of shale gas using fractal model and fuzzy theory: Evaluating fracturing heterogeneity, *Appl. Energy*, 250 (2019) 1246–1259. https://doi.org/10.1016/j.apenergy.2019.05.049.

[15] J. Lee, J. B. Rollins, J.P. Spivey, Pressure Transient Testing, Textbook Series, vol. 9, Society of Petroleum Engineers, Richardson, Texas, 2003.

[16] A. Araya, E. Ozkan, An Account of Decline-Type-Curve Analysis of Vertical, Fractured, and Horizontal Well Production Data, in Paper presented at the SPE Annual Technical Conference and Exhibition, San Antonio, Texas, September 2002. https://doi.org/10.2118/77690-MS.

[17] F. Medeiros, E. Ozkan, H. Kazemi, Productivity and Drainage Area of Fractured Horizontal Wells in Tight Gas Reservoirs, *SPE Reserv. Eval. Eng.*, 11 (5) (2008) 902–911. https://doi.org/10.2118/108110-PA.

[18] F. Medeiros, B. Kurtoglu, E. Ozkan, H. Kazemi, Analysis of Production Data From Hydraulically Fractured Horizontal Wells in Shale Reservoirs, *SPE Reserv. Eval. Eng.*, 13 (3) (2010) 559–568. https://doi.org/10.2118/110848-PA.

[19] R.O. Bello, R.A. Wattenbarger, Multi-Stage Hydraulically Fractured Shale Gas Rate Transient Analysi, in Paper presented at the SPE North Africa Technical Conference and Exhibition, Cairo, Egypt, February 2010. https://doi.org/10.2118/126754-MS.

[20] M. Nobakht, C.R. Clarkson, D. Kaviani, New type curves for analyzing horizontal well with multiple fractures in shale gas reservoirs, *J. Nat. Gas Sci. Eng.*, 10 (2013) 99–112. https://doi.org/10.1016/j.jngse.2012.09.002.

[21] M.S. Kanfar and R.A. Wattenbarger, Comparison of Empirical Decline Curve Methods for Shale Wells, in Paper presented at the SPE Canadian Unconventional Resources Conference, Calgary, Alberta, Canada, October 2012. https://doi.org/10.2118/162648-MS.

[22] L. Tan, L. Zuo, B. Wang, Methods of Decline Curve Analysis for Shale Gas Reservoirs, *Energies*, 11 (3) (2018) 552. https://doi.org/10.3390/en11030552.

[23] O. Mahmoud, M. Ibrahim, C. Pieprzica, L. Shane, EUR Prediction for Unconventional Reservoirs: State of the Art and Field Case, in Paper presented at the SPE Trinidad and Tobago Section Energy Resources Conference, Port of Spain, Trinidad and Tobago, June 2018. https://doi.org/10.2118/191160-MS.

[24] M. Ibrahim, O. Mahmoud, C. Pieprzica, A New Look at Reserves Estimation of Unconventional Gas Reservoirs, in Paper presented at the SPE/AAPG/SEG Unconventional Resources Technology Conference, Houston, Texas, USA, July 2018. https://doi.org/10.15530/URTEC-2018-2903130.

[25] H. Liang, L. Zhang, Y. Zhao, B. Zhang, C. Chang, M. Chen, M. Bai, Empirical methods of decline-curve analysis for shale gas reservoirs: Review, evaluation, and application, *J. Nat. Gas Sci. Eng.*, 83 (2020) 103531. https://doi.org/10.1016/j.jngse.2020.103531.

[26] A. Tadjer, A. Hong, R. Bratvold, Bayesian Deep Decline Curve Analysis: A New Approach for Well Oil Production Modeling and Forecasting, *SPE Reserv. Eval. Eng.*, (2022) 1–15. https://doi.org/10.2118/209616-PA.

[27] X. Li, X. Ma, F. Xiao, C. Xiao, F. Wang, S. Zhang, Small-Sample Production Prediction of Fractured Wells Using Multitask Learning, *SPE J.*, (2022) 1–16. https://doi.org/10.2118/209231-PA.

[28] H.S. Jha, A. Khanal, J. Lee, Statistical and Machine-Learning Methods Automate Multi-Segment Arps Decline Model Workflow to Forecast Production in Unconventional Reservoirs, in Paper presented at the SPE Canadian Energy Technology Conference, Calgary, Alberta, Canada, March 2022. https://doi.org/10.2118/208884-MS.

[29] M. Nobakht, L. Mattar, S. Moghadam, D.M. Anderson, Simplified Yet Rigorous Forecasting of Tight/Shale Gas Production in Linear Flow, in Paper presented at the SPE Western Regional Meeting, Anaheim, California, USA, May 2010. https://doi.org/10.2118/133615-MS.

[30] M. Nobakht, R. Ambrose, C. R. Clarkson, Effect of Heterogeneity in a Horizontal Well With Multiple Fractures on the Long-Term Forecast in Shale Gas Reservoirs, in Paper presented at the Canadian Unconventional Resources Conference, Calgary, Alberta, Canada, November 2011. https://doi.org/10.2118/149400-MS.

[31] J.J. Arps, Analysis of Decline Curves, *Trans. AIME*, 160 (1) (1945) 228–247. https://doi.org/10.2118/945228-G.

[32] R.H. Johnson, A.L. Bollens, The Loss Ratio Method of Extrapolating Oil Well Decline Curves, *Trans. AIME*, 77 (1) (1927) 771–778. https://doi.org/10.2118/927771-G.

[33] S.J. Pirson, Production Decline Curve of Oil Well May Be Extrapolated by Loss-Ratio, *Oil and Gas J.*, (1935).

[34] J.J. Arps, Estimation of Primary Oil Reserves, *Trans. AIME*, 207 (1) (1956) 182–191. https://doi.org/10.2118/627-G.

[35] D. Ilk, J.A. Rushing, A.D. Perego, T.A. Blasingame, Exponential vs. Hyperbolic Decline in Tight Gas Sands: Understanding the Origin and Implications for Reserve Estimates Using Arps' Decline Curves, in Paper presented at the SPE Annual Technical Conference and Exhibition, Denver, Colorado, USA, September 2008. https://doi.org/10.2118/116731-MS.

[36] P.P. Valkó, Assigning Value to Stimulation in the Barnett Shale: A Simultaneous Analysis of 7000 Plus Production Histories and Well Completion Records," in Paper presented at the SPE Hydraulic Fracturing Technology Conference, The Woodlands, Texas, January 2009. https://doi.org/10.2118/119369-MS.

[37] F.S. Huang, Y.S. Zhao, Q. N. Liu, A New Model for Oilfield Performance Prediction, *Petroleum Geology and Oilfield Development in Daqing*, 6 (4) (1987) 55–62.

[38] J. Hu, Y. Chen, Application and Discussion on T-Model, *Natural Gas Industry*, 15 (4) (1995) 26–29.

[39] H. Dou, C. Chen, Y. Chang, Y. Fang, X. Chen, W. Liu, W. Cai, Analysis and Comparison of Decline Models: A Field Case Study for the Intercampo Oil Field, Venezuela, *SPE Reserv. Eval. Eng.*, 12 (1) (2009) 68–78. https://doi.org/10.2118/106440-PA.

[40] A.J. Clark, L.W. Lake, T.W. Patzek, Production Forecasting with Logistic Growth Models, in Paper presented at the SPE Annual Technical Conference and Exhibition, Denver, Colorado, USA, October 2011. https://doi.org/10.2118/144790-MS.

[41] R.P. Spencer, M.J. Coulombe, Quantitation of Hepatic Growth and Regeneration, *Growth, Development and Aging*, 30 (3) (1966) 277–284.

[42] A.N. Duong, Rate-Decline Analysis for Fracture-Dominated Shale Reservoirs, *SPE Reserv. Eval. Eng.*, 14 (3) (2011) 377–387. https://doi.org/10.2118/137748-PA.

[43] S. Yu, D.J. Miocevic, An Improved Method to Obtain Reliable Production and EUR Prediction for Wells with Short Production History in Tight/Shale Reservoirs, in Paper presented at the SPE/AAPG/SEG Unconventional Resources Technology Conference, Denver, Colorado, USA, August 2013, pp. 29–39. https://doi.org/10.1190/urtec2013-003.

[44] H. Zhang, M. Cocco, D. Rietz, A. Cagle, An Empirical Extended Exponential Decline Curve for Shale Reservoirs, in Paper presented at the SPE Annual Technical Conference and Exhibition, Houston, Texas, USA, September 2015. https://doi.org/10.2118/175016-MS.

[45] M.J. Fetkovich, Decline Curve Analysis Using Type Curves, *J. Pet. Technol.*, 32 (6) (1980) 1065–1077. https://doi.org/10.2118/4629-PA.

[46] L. Mattar, S. Moghadam, Modified Power Law Exponential Decline for Tight Gas, in Paper presented at the Canadian International Petroleum Conference, Calgary, Alberta, June 2009. https://doi.org/10.2118/2009-198.

[47] K. Joshi, J. Lee, Comparison of Various Deterministic Forecasting Techniques in Shale Gas Reservoirs, in Paper presented at the SPE Hydraulic Fracturing Technology Conference, The Woodlands, Texas, USA, February 2013. https://doi.org/10.2118/163870-MS.

[48] N.T. Wang, Z.L. Chen, M.Q. Zhu, H. Zhu, Analysis of the combined model for the production decline of the shale-gas fractured horizontal well, *Pet. Geol. Oilfield Dev. Daqing*, 37 (5) (2018) 138–143. https://doi.org/10.19597/J.ISSN.1000-3754.201707046.

[49] Q. Chen, N. Wang, K. Ruan, M. Zhang, Selection of production decline analysis method of shale gas well, *Reserv. Eval. Develop*, 8 (2) (2018) 76–79. https://doi.org/10.13809/j.cnki.cn32-1825/te.2018.02.014.

[50] H.A. Al-Ahmadi, A.M. Almarzooq, R.A. Wattenbarger, Application of Linear Flow Analysis to Shale Gas Wells—Field Cases, in Paper presented at the SPE Unconventional Gas Conference, Pittsburgh, Pennsylvania, USA, February 2010. https://doi.org/10.2118/130370-MS.

[51] M. Ibrahim, R.A. Wattenbarger, Analysis of Rate Dependence in Transient Linear Flow in Tight Gas Wells, in Paper presented at the Canadian International Petroleum Conference, Calgary, Alberta, June 2005. https://doi.org/10.2118/2005-057.

[52] Society of Petroleum Engineers, Datasets. https://www.spe.org/datasets/, 2021 (accessed 30 December 2021).